

# Microstructural Characterization of IN617 and DMV617 Mod Alloys after Long-Time Aging at 700 °C †

Iwona Bednarczyk <sup>1,\*</sup>, Kinga Rodak <sup>1,\*</sup> , Adam Hernas <sup>1</sup> and Vlastimil Vodárek <sup>2</sup>

<sup>1</sup> Faculty of Materials Engineering, Silesian Technical University, Akademicka 2A, 44-100 Gliwice, Poland; iwona.bednarczyk@polsl.pl (I.B.); adam.hernas@polsl.pl (A.H.)

<sup>2</sup> Faculty of Materials Science and Technology, VŠB—Technical University of Ostrava, 17. Listopadu 15, 708 33 Ostrava, Czech Republic; vlastimil.vodarek@vsb.cz

\* Correspondence: kinga.rodak@polsl.pl

† Presented at the 30th International Conference on Modern Metallurgy—Iron and Steelmaking, Kosice, Slovakia, 27–29 September 2023.

**Abstract:** In the present paper, microstructural changes in two alloys, IN617 and DMV617 mod, after 5 h and 1000 h of aging at 700 °C were investigated using scanning transmission electron microscopy. The mechanical properties of the samples were evaluated using hardness tests. Precipitates were identified using energy-dispersive X-ray spectroscopy analysis. After long-term aging, intensive precipitation of the  $M_{23}C_6$  carbides and  $\gamma'$  intermetallic phase in the microstructure of alloys was observed. In the IN617 alloy, continuous layers of  $M_{23}C_6$  carbides along the grain boundaries after long-term aging were observed. The minor addition of boron to the DMV617 mod alloy is advantageous in microstructure formation during long-term aging because it decreases the agglomeration of  $M_{23}C_6$  at the grain boundaries.

**Keywords:** IN617 and DMV617 mod alloys; heat treatment; microstructure; phase precipitation; scanning transmission electron microscopy



**Citation:** Bednarczyk, I.; Rodak, K.; Hernas, A.; Vodárek, V. Microstructural Characterization of IN617 and DMV617 Mod Alloys after Long-Time Aging at 700 °C. *Eng. Proc.* **2024**, *64*, 12. <https://doi.org/10.3390/engproc2024064012>

Academic Editors: Branislav Bul'ko, Dana Baricová, Peter Demeter and Róbert Dzurňák

Published: 26 February 2024



**Copyright:** © 2024 by the authors. Licensee MDPI, Basel, Switzerland. This article is an open access article distributed under the terms and conditions of the Creative Commons Attribution (CC BY) license (<https://creativecommons.org/licenses/by/4.0/>).

## 1. Introduction

The legal and ecological conditions of the country and the EU require the construction of ultra-supercritical power units with high efficiency (above 46%) and lower emissions of harmful  $SO_x$ ,  $NO_x$ , and  $CO_2$  compounds into the atmosphere. Increasing the steam temperature to approximately 700 °C and the pressure to over 30 MPa requires the use of materials that must be characterized by high creep resistance and structural stability at high temperatures. One of the nickel superalloys that can be used for boiler pressure elements is Inconel Alloy617 (NiCr23Co12Mo). This alloy is characterized by good mechanical properties at elevated temperatures and resistance to corrosion and oxidation in aggressive environments [1–3]. The new DMV617 mod alloys contain additional B and N in their chemical compositions. These additives cause a more favorable set of functional properties [4,5]. In the present paper, the changes in the structure of IN617 and DMV617 mod alloys after aging at a temperature of 700 °C and a heating time of 5 h and 1000 h are investigated [6].

All elements included in Ni-based alloys can be divided into three basic groups. The first group consists of elements forming the alloy matrix, such as Co, Fe, Cr, Mn, Si, and Mo. Group II includes elements forming the  $\gamma'$  phase, such as Ni, Al, and Ti. Group III includes C and B. Ni, which is the basic component of the alloys, determines their structure and phase stability. The addition of Cr and Si ensures the matrix's resistance to oxidation at elevated temperatures. By forming carbides  $M_{23}C_6$  with high durability, Cr also affects the creep strength and plastic properties of superalloys [7,8]. Al and Ti are added to strengthen the superalloy by precipitating the  $\gamma'$  phase. Fe can partially replace Ni in the matrix, which causes the alloy to become cheaper, but as the content of this element increases, the

heat resistance decreases due to the lower adhesion of the oxidized layers containing iron oxides. As the Fe content increases, the susceptibility of Ni alloys to the precipitation of the unfavorable  $\sigma$  phase also increases [8]. Co, which can also constitute an alloy matrix, when added to Ni alloys, significantly reduces the solubility of elements such as Al and Ti in the matrix. These elements increase the alloys' heat resistance. Mo is introduced into alloys mainly to strengthen the solid solution at elevated temperatures. This element also forms carbides, mainly complex ones, often containing additional Cr and Fe. The presence of this element in the  $\gamma'$  phase increases its strengthening properties.

## 2. Materials and Methods

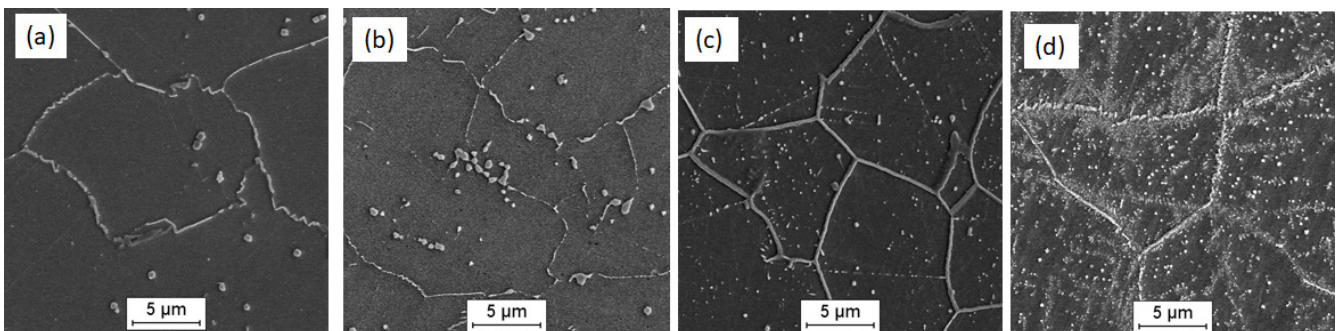
The materials for investigation were IN617 and DMV617 mod alloys after saturation. The chemical composition (Table 1) of the DMV617 mod alloy was modified with the microaddition of B and N; moreover, the Si and Fe content was limited. The alloy aging process was carried out at a temperature of 700 °C and heated for 5 h and 1000 h with cooling in a furnace. A Hitachi HD-2300A scanning transmission electron microscopy (STEM) technique was used for microstructural investigation. Energy dispersive X-ray spectroscopy (EDS) analysis of the precipitates was performed on thin foils and extraction replicas. Quantitative analysis of the  $\gamma'$  phase precipitates (average diameter) was performed based on images recorded on a STEM using the Metilo program [9].

**Table 1.** Chemical composition of alloys.

Alloy	C	Cr	Co	Mo	Al	Ti	Mn	Si	Fe	B	N	Ni
IN617	0.1	22.0	12.0	9.0	1.0	0.4	0.7	0.7	2.0	-	-	Bal.
DMV617 mod	0.1	22.0	12.0	9.0	1.0	0.4	0.7	0.3	1.5	0.01	0.05	Bal.

## 3. Results and Discussion

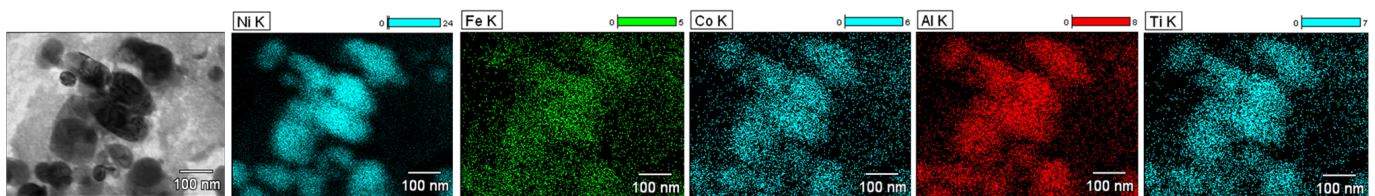
The initial microstructure of the alloy consists of prior austenite grains. In this state,  $M_{23}C_6$  and MC(X) carbides are distributed along the grain boundaries and inside the grains [6]. The microstructure of the alloys after aging at 700 °C/5 h and 700 °C/1000 h is presented in Figure 1. Three kinds of precipitates are identified in both alloys by EDS analysis:  $M_{23}C_6$ , MC(X), and the  $\gamma'$  intermetallic phase (Table 2). From the obtained results in Figure 1, it is evident that  $M_{23}C_6$  and MC(X) carbides are well visible within the grains and at the grain boundaries. Studies conducted showed that the  $\gamma'$  phase was observed after the aging process (Figure 2). However, the amount of the  $\gamma'$  phase in the IN617 and DMV617 mod alloys during 5 h of aging at 700 °C was slight and not well visible in thin foil; for this reason, EDX investigations were performed using extraction replicas methods.



**Figure 1.** SEM images of (a) IN617 after aging at 700 °C/5 h, (b) IN617 after aging at 700 °C/1000 h, (c) DMV617 mod after aging at 700 °C/5 h, and (d) DMV617 mod after aging at 700 °C/1000 h.

**Table 2.** Chemical composition of precipitates in IN617 and DMV 617 mod after aging.

IN617 (700 °C/5 h)	Chemical Composition (wt.%)						
	Ni	Cr	Co	Mo	Al	Fe	Ti
M <sub>23</sub> C <sub>6</sub>	13	60	6	20	-	1	-
γ'	72	3	-	9	12	2	2
γ	54	21	13	10	-	2	-
IN617 (700 °C/1000 h)							
M <sub>23</sub> C <sub>6</sub>	5	72	2	21	-	-	-
γ'	74	4	-	7	10	1	4
γ	60	23	1	10	3	3	-
DMV617 mod (700 °C/1000 h)							
M <sub>23</sub> C <sub>6</sub>	7	72	2	19	-	-	-
γ'	79	1	3	3	5	4	5
γ	58	20	12	9	-	1	-

**Figure 2.** STEM-EDS mapping of the γ' phase in the DMV617 mod alloy after aging at 700 °C/1000 h.

The solid solution based on Ni is characterized by high heat resistance. This significant increase in the heat resistance of Ni is caused by its significant susceptibility to creating solid solutions with high stability [7,8]. The strengthening of the solid solution γ is mainly provided by the alloying elements dissolved in it, which reduce the diffusion coefficient and the stacking fault energy, making transverse slip more difficult [7]. Based on the XRD analysis of the investigated alloys, it was shown that the elements that have a particularly intensive impact on the strengthening of the matrix are Ni, Co, Fe, Cr, Mo, and Al to a lesser extent (see Table 2). However, the average metallic composition of the matrix of the investigated alloys varies.

The γ' phase has a decisive influence on the heat resistance [7,8]. Due to long-term aging, decomposition of the solid solution γ occurs, and the heat resistance and plasticity of the alloy significantly decrease. The amount of the precipitated phase depends primarily on the total content of Al and Ti in the alloy because the chemical composition of this phase has a significant impact on its morphology and properties. Based on the XRD analysis of the investigated alloys, it was shown that the elements that have a particularly intensive impact on the strengthening of the γ' are Ni, Co, Fe, Cr, Mo, and Al (see Table 2 and Figure 2). The chemical composition of the γ' phase also affects the degree of coherency of its crystal lattice to the matrix lattice, which affects the morphology of the precipitates [7,8]. Its strengthening effect is greatest when the mutual coherence of the matrix and the γ' phase is ensured (Figure 3). With the increase in aging time, γ' shows no coherence with the matrix. At the same time, the phase size and shape change. In the IN617 alloy, the average diameter of the γ' phase is 11.7 nm and 58.1 nm, respectively, for 5 h and 1000 h of aging. Meanwhile, in the DMV617 alloy, the average diameter of the γ' phase after 1000 h of aging is 71.1 nm. The γ' particles for 5 h of aging were not observed in the extracted replicas.

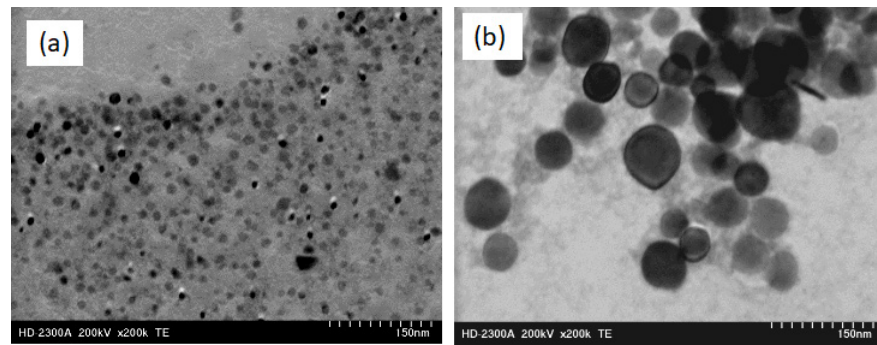


**Figure 3.** Microstructure of the extracted  $\gamma'$  phase in the IN617 alloy: (a) 700 °C/5 h and (b) 700 °C/1000 h.

$M_{23}C_6$  carbide, characteristic of Ni alloys, is released during heat treatment as a result of Cr binding C from the matrix. In the investigated alloys,  $M_{23}C_6$  carbide approximately corresponds to the formula Cr, (Mo, Ni, Co, Fe) C (Table 2). An important change in the microstructure is the increase in the volume fraction of carbides with increasing aging time (Figures 1, 4 and 5). Initially, carbides are formed as discrete particles along the grain boundaries, and then, with increasing time, they continue to be formed as continuous phases along the grain boundaries, twin boundaries, and as scattered particles within the grains (for example, Figure 1a). The continuous network of carbides (visible in Figure 1c) at the grain boundaries facilitates the propagation of cracks, and the difficult sliding process along the grain boundaries affects the stress concentration and accelerates the occurrence of brittle scrap. On the other hand, if there are no carbides at the grain boundaries, the boundary slipping is facilitated by the simultaneous occurrence of voids during plastic deformation at elevated temperatures [7,8].

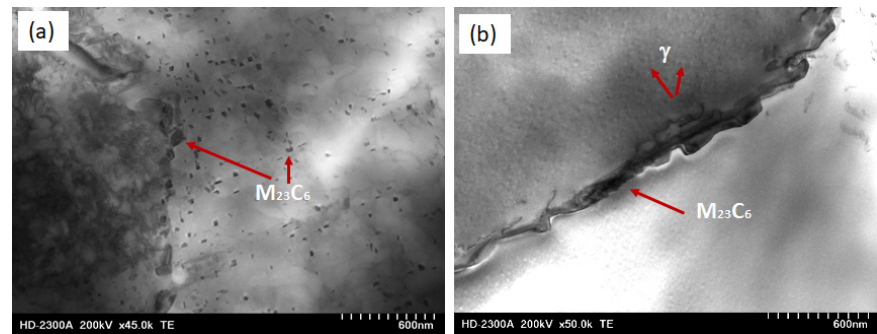


**Figure 4.**  $M_{23}C_6$  carbides and the  $\gamma'$  phase in (a) the IN617 alloy after aging at 700 °C/5 h and (b) the DMV617 mod alloy after aging at 700 °C/5 h.

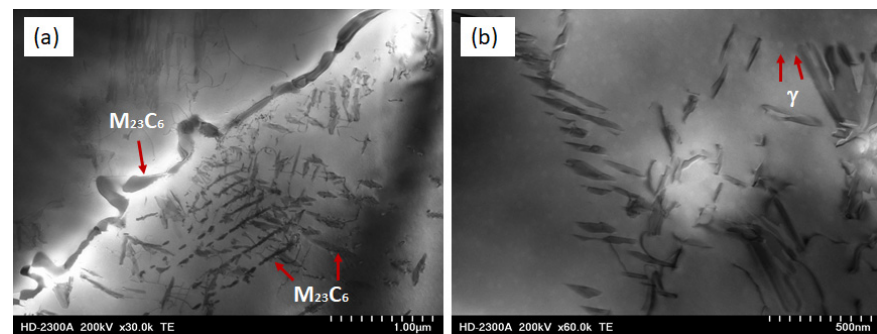


**Figure 5.**  $M_{23}C_6$  carbides (a) and the  $\gamma'$  phase (b) in the DMV617 mod alloy after aging at 700 °C/1000 h.

The carbide mesh visible in DMV617 mod during aging at 700 °C/5 h (Figure 1c) “disappears” during long-term aging (Figures 1d, 4 and 5). The particularly harmful effect

of the “mesh”  $M_{23}C_6$  particles on grain boundaries can be removed by the release of the  $\gamma'$  phase at the grain boundaries, blocking the growth of  $M_{23}C_6$  [5]. Inside the grains, small carbides with a plate-like and rod-like shape are observed after long-term aging (Figure 5). The small  $M_{23}C_6$  carbides are especially responsible for the pinning of dislocation during creep. It should be noted that the morphology of carbide precipitates during the aging of both alloys is different. In the IN617 alloy, carbides are precipitated along the grain boundaries and further grow along the grain boundaries with the extension in the aging time. However, in the DMV617 mod alloy, the secondary phases are more fragmented and evenly distributed in the matrix, which is undoubtedly influenced by the microaddition of B. Increasing the aging temperature results in an intensified  $M_{23}C_6$  carbide release.

The hardness of the alloys starts to increase as the aging time increases (Figure 6). Moreover, the hardness of the DMV617 mod alloy becomes less than that of the IN617 alloy. The changes in hardness values are consistent with microstructural changes in the samples. The precipitation of the  $M_{23}C_6$  carbides promotes the depletion of Mo, Ni, Cr, and Fe from the solid solution. On the other hand, the  $M_{23}C_6$  carbides can contribute to the increase in the strength through precipitation hardening. From the literature, it is known [8] that precipitation strengthening can compensate for the loss of solid solution at an early stage of aging where the particles of carbides are small. After a long aging period, the  $M_{23}C_6$  precipitates lose their ability to inhibit the motion of dislocations. Such interplay between the solid solution strengthening and precipitation strengthening also applies to the  $\gamma'$  phase. It is interesting to note that the average diameter of the  $\gamma'$  phase in the DMV617 mod alloy is bigger than in the IN617 alloy.

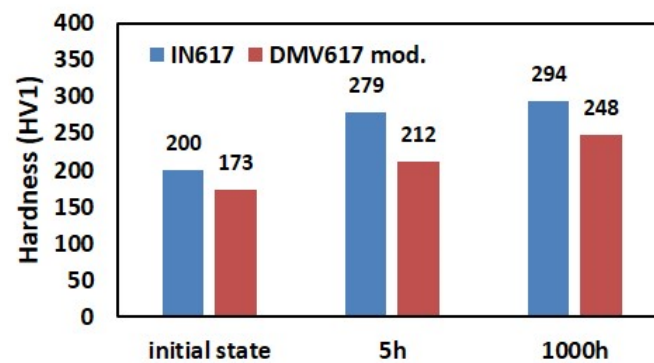


Figure 6. Influence of chemical composition and aging time on changes in hardness.

#### 4. Summary

The pronounced precipitation of the  $M_{23}C_6$  carbides and the  $\gamma'$  intermetallic phase in alloys takes place during long-term aging.  $M_{23}C_6$  carbides frequently precipitate on grain boundaries and inside grains. Different morphologies of  $M_{23}C_6$  carbides were detected in the analyzed alloys. Particles with irregular shapes were observed, especially at the grain boundaries of the IN617 alloy. Meanwhile, in the DMV617 mod alloy, the carbides in the grain boundaries were smaller and more regular. Moreover, inside the grain, regular and equiaxed carbides were observed. As the aging time increased, the average diameter of the  $\gamma'$  phase increased in both phases. In the DMV617 mod alloy, the growth of the  $\gamma'$  phase was greater than in the IN617 alloy.

**Author Contributions:** Conceptualization: K.R.; methodology: K.R. and I.B.; validation: K.R.; formal analysis: K.R. and I.B.; investigation: K.R. and I.B.; writing—original draft preparation: K.R. and I.B.; writing—review and editing: K.R.; supervision: A.H. and V.V. All authors have read and agreed to the published version of the manuscript.

**Funding:** This research was funded by the National Centre of Research and Development, grant number SP/E/1/67484/10.

**Institutional Review Board Statement:** Not applicable.

**Informed Consent Statement:** Not applicable.

**Data Availability Statement:** The raw and processed data used to achieve the findings of this work are not currently available for public sharing as they are part of a bigger research program.

**Conflicts of Interest:** The authors declare no conflicts of interest.

## References

1. Zhao, S.; Xie, X.; Smith, G.D.; Patel, J. Microstructural stability and mechanical properties of a new nickel-based superalloys. *Mater. Sci. Eng. A* **2003**, *355*, 96–105. [[CrossRef](#)]
2. Shingledecker, J.P.; Swindeman, R.W.; Wu, Q.; Vasudevan, V.K. Creep Strength of High-Temperature Alloys for USC Steam Boilers. In Proceedings of the 4th International Conference on Advances in Materials Technology for Fossil Power Plants, Hilton Head, SC, USA, 25–28 October 2004; ASM-International: Materials Park, OH, USA, 2005.
3. Xie, X.; Zhao, S.; Dong, J.; Smith, G.D.; Baker, B.A.; Patel, S.J. Modification of Ni-Cr-Co-Mo-Nb-Ti-Al Superalloy for USC Power Plant Application at Temperature above 750 °C. *Mater. Sci. Forum* **2007**, *561–565*, 471–476. [[CrossRef](#)]
4. Kontis, P.; Mohd Yusof, H.A.; Pedrazzini, S.; Danaie, M.; Moore, K.L.; Bagot, P.A.J.; Moody, M.P.; Grovenor, C.R.M.; Reed, R.C. On the effect of boron on grain boundary character in a new polycrystalline superalloy. *Acta Mater.* **2016**, *103*, 688–699. [[CrossRef](#)]
5. Xie, W.; Wu, D.; Lu, S. Effects of boron addition on the microstructure and creep properties of a Ni-Fe-based superalloy weld metal alloy. *Mater. Res. Express* **2022**, *9*, 026522. [[CrossRef](#)]
6. Hernas, A.; Dobrzański, J.; Pasternak, J.; Fudali, S. *Charakterystyki Nowej Generacji Materiałów dla Energetyki*; Wydawnictwo Politechniki Śląskiej: Gliwice, Poland, 2015.
7. Wu, Q.; Song, H.; Swindeman, R.W.; Shingledecker, J.P.; Vasudevan, V.K. Microstructure of Long-Term Aged IN617 Ni-Base Superalloy. *Metall. Mater. Trans. A* **2008**, *39A*, 2569–2585. [[CrossRef](#)]
8. Di Martino, S.F.; Faulkner, R.G.; Hogg, S.C.; Vujic, S.; Tassa, O. Characterisation of microstructure and creep properties of alloy 617 for high-temperature applications. *Mater. Sci. Eng. A* **2014**, *619*, 77–86. [[CrossRef](#)]
9. Szala, J. *Application of Computer Picture Analysis Methods to Quantitative Assessment of Structure in Materials*; Scientific Journals of Silesian University of Technology, Series Metallurgy; Silesian University of Technology: Gliwice, Poland, 2008.

**Disclaimer/Publisher's Note:** The statements, opinions and data contained in all publications are solely those of the individual author(s) and contributor(s) and not of MDPI and/or the editor(s). MDPI and/or the editor(s) disclaim responsibility for any injury to people or property resulting from any ideas, methods, instructions or products referred to in the content.